Polar Biol (2005) 29: 27–39
DOI 10.1007/s00300-005-0032-2

ORIGINAL PAPER

A. Corzo · S. Rodríguez-Gálvez · L. Lubian · C. Sobrino
P. Sangrá · A. Martínez

Antarctic marine bacterioplankton subpopulations discriminated by their apparent content of nucleic acids differ in their response to ecological factors

Received: 3 January 2005 / Revised: 7 June 2005 / Accepted: 12 June 2005 / Published online: 17 August 2005

Abstract Bacterial abundances determined in Drake Passage and Bransfield and Gerlache Straits (Antarctica) in the Austral summer ranged from 0.78 to 9.4×10^5 cells ml^{-1}, and were positively correlated with standing stocks of Chl *a*. Two bacterial subpopulations were discriminated based in their different levels of green fluorescence and wide angle light scatter (SSC) per cell after SYTO-13 staining for the first time in Antarctic waters. High nucleic acid (HNA) and low nucleic acid (LNA) subpopulations differed considerably in their response to changes in environmental variables. The apparent content of nucleic acids per cell for the HNA subpopulation (FL1-HNA) showed vertical profiles similar to those of Chl *a*, including the presence of a maximum at the subsurface chlorophyll maximum. FL1-HNA was positively correlated with Chl *a*. No similar trends were observed for the LNA fraction. HNA and LNA subpopulations differed in the response of the wide angle light scatter signal to environmental factors as well. SSC-HNA decreased strongly with depth and was positively correlated with Chl *a*. Again, no similar trends were observed for the LNA subpopulation. The percentage of HNA cells (%HNA) ranged between 35.0 and 76.7% and showed a general tendency to increase with depth. This increase seemed to be larger when the stratification of the water column was higher. Differences in grazing pressure could be responsible of the unexpected vertical distribution of HNA cells. Our results shows that in situ LNA and HNA bacterioplankton subpopulations are under different ecological controls and likely to play different trophodynamic roles in Antarctic waters.

A. Corzo (✉)
Departamento de Biología,
Facultad de Ciencias del Mar y Ambientales,
Universidad de Cádiz, Polígono Río San Pedro,
11510 Puerto Real, Spain
E-mail: alfonso.corzo@uca.es
Tel.: +34-956-016177
Fax: +34-956-016019

S. Rodríguez-Gálvez · L. Lubian · C. Sobrino
Instituto de Ciencias Marinas de Andalucía (CSIC),
Polígono Río San Pedro, 11510 Puerto Real, Spain

P. Sangrá · A. Martínez
Departamento de Física, Campus Universitario de Tafira,
Edificio de Ciencias Básicas,
35017 Las Palmas de Gran Canaria, Spain

Introduction

Flow cytometry has been used to detect and characterise heterotrophic planktonic bacteria after staining them with fluorescent dyes at least since 1985 (Tyndall et al. 1985; Gasol and del Giorgio 2000). Either using UV-excitable or blue light-excitable stains, it is usually possible to find at least two bacterial subpopulations that differ considerably in the degree of staining and, therefore, in the nucleic acid content per cell (Robertson and Button 1989; Monger and Landry 1993; Li et al. 1995). These bacterial subpopulations have been found in both marine (Monger and Landry 1993; Li et al. 1995; Marie et al. 1997; Gasol et al. 1999) and fresh water environments (Button et al. 1996). They have been named in different ways (Li et al. 1995; Jacquet et al. 1998; Gasol et al. 1999). We call then high nucleic acid (HNA) and low nucleic acid (LNA) subpopulations according to Lebaron et al. (2001). Available evidence suggests that total cell fluorescence in SYTO-13 stained bacteria depends on both DNA and RNA cell content, being the contribution of each of them different with culture growth stage (Troussellier et al. 1999; Guindulain and Vives-Rego 2002).

The experimental evidence suggests that the HNA and LNA subpopulations differ considerably in growth rate, activity and in their relationship with others ecological variables. However, recent work suggests that both subpopulations were composed of the same dominant species (Servais et al. 2003; Longnecker et al.

2005). HNA cells from natural marine communities and from mesocosm experiments grew faster and presented higher rates of radioactive leucine and thymidine uptake than LNA cells (Li et al. 1995; Servais et al. 1999; Gasol and del Giorgio 2000; Servais et al. 2003). Abundances of HNA cells were positively correlated with total bacterial production (Lebaron et al. 2001). On individual cell basis leucine uptake was increased with both light scatter and fluorescence per cell (Lebaron et al. 2002). Few field studies deal with changes of both subpopulation in response to ecological factors. However, these have shown that the fluorescence level of HNA (the apparent content of nucleic acid), the difference respect to LNA and the HNA percentage respect to total bacterial population (%HNA) were positively correlated with chlorophyll concentration (Li et al. 1995), and the apparent nucleic acid content per cell and %HNA decreased with depth in Bedford Basin (Jellet et al. 1996). Both papers supported the notion that %HNA could be used as an index of bacterial growth (index of active cells). For ecological studies, the capacity of flow cytometry to quantify separately the active and less-active subpopulations is very promising because clearly both kinds of cells do not play the same role in the trophodymamics of the aquatic media. For instance, bacterial grazers seem to crop selectively the more active and larger cells of the bacterial community (Sherr et al. 1992; Jürgens and Güde 1994; Gasol et al. 1995).

Field data on the pattern of temporal and spatial variation of HNA and LNA fractions of the total heterotrophic bacterial community are very scarce. Similarly, little is known about the way in which the abundance of both subpopulations, their physiological characteristics, and level of activity are related to other key ecological variables in aquatic ecosystems. The main objectives of the present work were: (1) to test the presence of the HNA and LNA heterotrophic bacterial subpopulations in the Southern Ocean, where they have not been previously described; (2) to characterise the "flow cytometric signature" of the HNA and LNA subpopulations, regarding side scatter and fluorescence signals, in Antarctic waters; and (3) to analyse the differences in the response of both subpopulations to several ecological variables like chlorophyll concentration, depth and water column stratification. These objectives were addressed during the oceanographic cruise CIEMAR (1999–2000), in Drake Passage, and Bransfield and Gerlache Straits, where we analysed total bacterial numbers and the HNA and LNA subpopulations by flow cytometry after staining with SYTO-13.

Material and methods

Study area and sample collection

Sea water samples were collected during the oceanographic cruise CIEMAR 99/00 (BIO-Hespérides) carried out from 13 December 1999 to 3 January 2000. The study area was located in the Passage of Drake, Strait of Bransfield and Strait of Gerlache (Fig. 1). Samples were taken from 5, 10, 25, 50, 75, 100 m and the fluorescence maximum depth by means of a rosette system of 24 oceanographic 12 l Niskin bottles, operated through a General Oceanics MKIIIC CTD that also provided continuous vertical hydrographic information in real-time (temperature, salinity and fluorescence).

Flow cytometry

Bacterioplankton fresh samples from each depth were stained with SYTO-13 and analysed by flow cytometry on board, immediately after collection. The method of del Giorgio et al. (1996a) was followed. Briefly, 2.5 µl of a solution of SYTO-13 (Molecular Probes) dissolved in dimethyl sulfoxide was added to 500 µl of water samples to obtain a final concentration of 2.5 µM SYTO-13. After vigorous shaking, the samples were incubated during 10 min at room temperature in the dark, followed by the addition of 10 µl of a yellow-green autofluorescent microspheres solution FluoSpheres carboxylated-modified microspheres, 1.0 µm) of known concentration to stained samples as internal standard for instrument performance. After shaking, the samples were immediately analysed in a FACScalibur flow cytometer (Becton Dickinson). Since their concentration was known, the volume of sample processed could be calculated and therefore the abundance of bacteria per unit of volume. The flow cytometer settings for the analysis of these samples were established as follows: Photodetectors gains in logarithmic amplification were FSC = E-02, SSC = 470, FL1 = 450, FL2 = 475, FL3 = 590. Threshold was set at FL1 = 72, therefore, only particles with green fluorescence (apparent nucleic acid content) larger than that level were recorded. MilliQ water was used as sheath fluid. Flow rate of sample through the flow chamber was set at low rate (12 ± 3 µl min^{-1}) and calibrated several times during the cruise. This flow rate and the mean concentration of bacteria found in this study determined a conveniently low particle passage rate generally lower than 300 events s^{-1} . Data were acquired with the software CellQuest as Flow Cytometry Standard files and later analysed with CellQuest and Attractor software (Becton Dickinson). Stained bacteria were discriminated and counted in a bivariate plot of right angle light scatter (SSC) and green fluorescence (FL1) measured at 530 ± 30 nm. The FL1 and SSC signals from bacteria were normalised by dividing the corresponding microspheres signals in each sample. HNA and LNA cells were easily discriminated, gated and counted in the same plot.

The presence of autotrophic picoplankton in a size range close to bacteria may complicate the quantification of heterotrophic bacteria. However, photosynthetic prokaryotic picoplankton were essentially absent during the CIEMAR cruise (Rodríguez et al., in prep.).

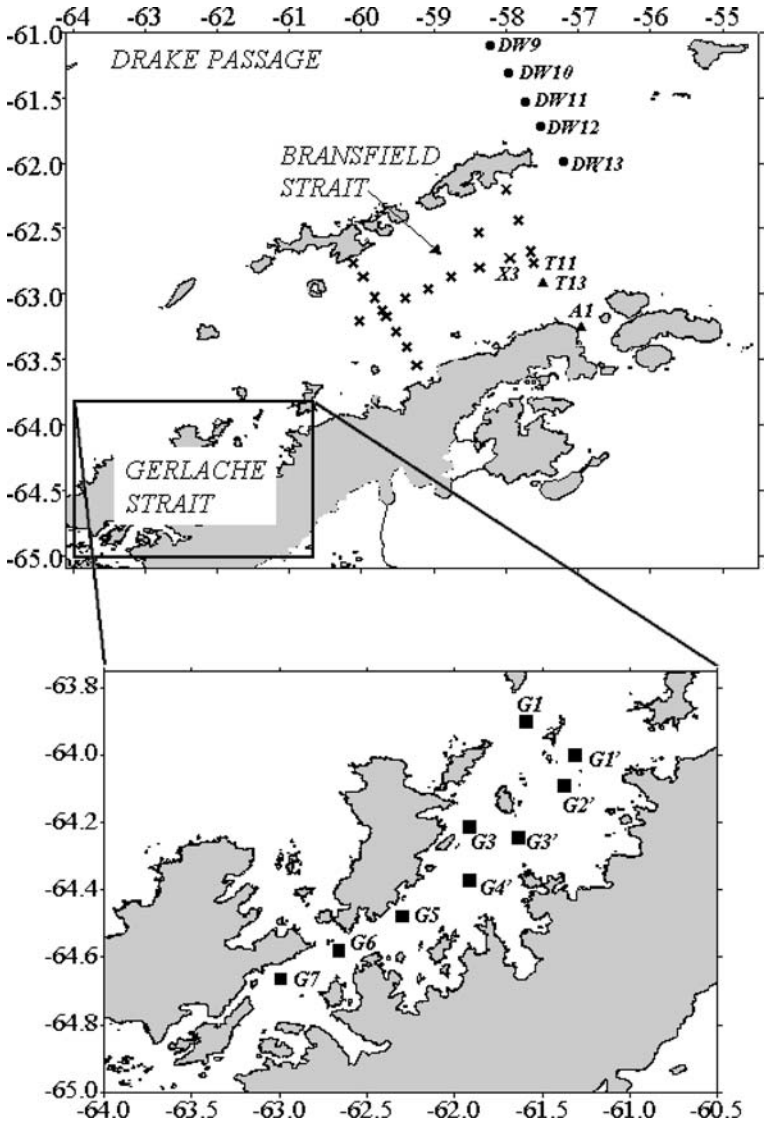

Fig. 1 Map of the study region. Due to the large horizontal heterogeneity of the studied area we have distinguished 4 zones. Drake Passage, Transitional Zonal Water with Bellingshausen Sea influence (TBW) localised in the northern part of the Bransfield Strait, Transitional Zonal Water with Weddell Sea influence (TWW) localised in the southern and Gerlache Strait. Numbered stations were sampled for physical and biological variables, the rest were sampled only for physical variables and in situ fluorescence

Likewise, very low abundances of photosynthetic prokaryotic picoplankton were observed in Gerlache Strait (Rodríguez et al. 2002).

Chlorophyll and inorganic nutrients

Chlorophyll *a* (Chl *a*) was determined fluorimetrically following the method of Yentsch and Menzel (1963) modified by Holm-Hansen et al. (1965). Samples (1 l) were filtered through Whatman GF/F filters and extracted overnight in 5 ml 90% acetone at 4 °C in dark. Fluorescence was measured before and after acidification with a fluorometer (Turner Designs 10) calibrated with pure Chl *a* (Sigma) following UNESCO (1994). Samples for inorganic nutrients (nitrate, nitrite, phosphate and silicate) were stored frozen (−20 °C) until analysis by means of a Traacs 800 Bran Luebbe autoanalyser following standard protocols (Grasshoff et al. 1983).

Results

Hydrography

Based on previous studies and on our own hydrographic data we have differentiated four areas (Figs. 1, 2). In Bransfield Strait, it is generally accepted the distinction between the Transitional Zonal Water with Bellingshausen Sea influence (TBW) localised in the northern part of the strait and the Transitional Zonal Water with Weddell Sea influence (TWW) localised in the southern part. TBW is a relatively warm and low-salinity water mass, which flows into the Bransfield basin from the west, while TWW is a cooler and salty inflow from the Weddell Sea. Both water masses also differed in the degree of stratification as suggested by their potential density profiles (Fig. 2). The contact between both water masses creates the Bransfield Front following a Southeast–Northwest direction (García et al. 2002). During the CIEMAR cruise in 1999,

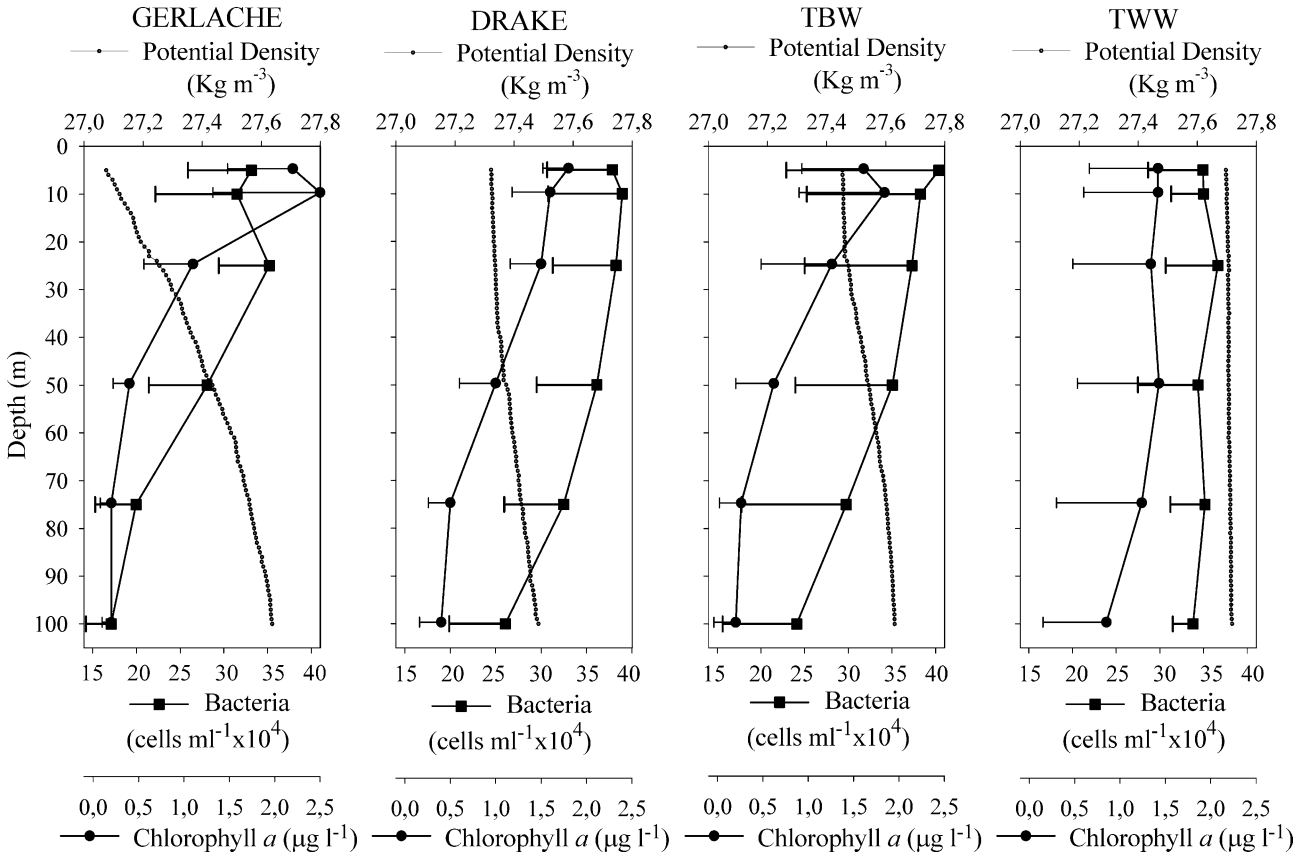

Fig. 2 Mean potential density, mean chlorophyll *a* (µg l^{-1}) and mean total bacterial abundance (Bacteria ml^{-1}) profiles for Gerlache Strait, Drake Passage, TBW and TWW zones. SD represented as a single arm bar for clarity sake

however, we found a different hydrographic situation (Corzo et al. 2005; Sangrá et al. in prep). At the time of sampling the surface waters in most of the strait presented physicochemical properties considered typical of TBW. In fact, the Bransfield Front was only detectable in the eastern transect between stations T11 and T13 and it was not detected in the western transect in surface (Fig. 1). Since we will deal only with the upper 100 m of the water column, all biologically sampled Bransfield stations have been considered dominated by TBW. The only exceptions were stations T13 and A1, which clearly presented physicochemical characteristics more typical of TWW, with higher and uniform potential density (Fig. 2). The third and fourth areas included a transect in Drake Passage and two transects in the Gerlache Strait, respectively. The higher degree of stratification was found in the Gerlache Strait as shown by the mean vertical profile of potential density (Fig. 2). A more detailed hydrographic description will be reported elsewhere (Sangrá et al. in prep.).

Autotrophic biomass and total bacterial abundance

Integrated chlorophyll concentration for the upper water column (0–100 m) ranged between 32.0 and 189.8 mg Chl *a* m^{-2}. The highest integrated concentration of autotrophic biomass as estimated by Chl *a* was found in Southeastern Bransfield Strait, in coastal waters close to the Antarctic Peninsula (station A1). The lowest value was found close to the Bransfield front in Western Bransfield Strait (station X3). The horizontal distribution of Chl *a* was very heterogeneous as estimated by the coefficient of variation (CV) between stations (40%) (Table 1). Horizontal heterogeneity in each of the fourth zones discriminated in our study was also high (20.8–66.4%). Gerlache Strait and Drake Passage were found to be more homogeneous. The mean vertical profile of Chl *a* for the whole area showed a subsurface maximum at 10 m (2.00 ± 0.99µg l^{-1}). The subsurface chlorophyll maximum was very clear in Gerlache Strait and TBW, where the water column was more stratified according to the potential density profiles, but it was absent or less pronounced in the more homogeneous water columns of Drake Passage and the TWW zone (Fig. 2).

Total bacteria ranged between 7.8×10^4 and 9.4×10^5 cell ml^{-1} . Mean total bacterial abundances for the four zones decreased with depth, although a subsurface maximum was observed at 25 m in Gerlache Strait and TWW zone in the average profiles (Fig. 2). Integrated abundance of total heterotrophic bacteria per unit of area showed less horizontal heterogeneity than Chl *a* as estimated by the CV among all stations (23%). Integrated total bacterial abundances in TBW, TWW and Drake Passage were not significantly different but were significantly higher than those found in the Strait of

Table 1 Average values and coefficient of variation (CV, %) of chlorophyll standing stocks (Chl *a*), total heterotrophic bacteria (Bacteria) and %HNA integrated for the upper 100 m in the four zones

	Chl a (CV) mg m^{-2}	Bacteria (CV)×10^{13} m^2	%HNA (CV)	Number of stations
TBW	80.8 (41.3)	3.47 (24.7)	57.96 (12.9)	19
TWW	129.1 (66.4)	3.53 (13.5)	64.08 (3.6)	2
Gerlache	76.8 (20.8)	2.66 (13.8)	69.93 (6.8)	9
Drake	98.4 (25.4)	3.35 (9.1)	60.94 (9.0)	5
All zones	84.55 (40.0)	3.31 (28)	62.20 (13.1)	35

TBW Transitional Zonal Water with Bellingshausen Sea influence, *TWW* Transitional Zonal Water with Weddell Sea influence, Gerlache Strait and Drake Passage

Table 2 Linear regression between the abundance of heterotrophic bacteria (y) and chlorophyll *a* (x) for different zones. Both variables were log-transformed. In the equations, the standard error of the intercept and slope are represented in brackets. Determination coefficient (r^2), number of samples (n), and p-value (p) are shown as well

Zone	Equation	r^2	n	p
Drake	$y = 5.539(0.014) + 0.196(0.046)x$	0.406	28	< 0.01
Bransfield-TBW	$y = 5.574(0.012) + 0.152(0.021)x$	0.313	115	< 0.01
Bransfield-TWW	$y = 5.554(0.013) - 0.123(0.021)x$	0.315	13	< 0.05
Gerlache	$y = 5.461(0.017) + 0.198(0.030)x$	0.406	66	< 0.01
All	$y = 5.533(0.009) + 0.163(0.017)x$	0.290	222	< 0.01

Gerlache (*t*-student, $\alpha = 0.05$), where integrated Chl *a* was also lower (Table 1). Abundance of heterotrophic bacteria was significantly and positively correlated with Chl *a* in Gerlache, Drake and TBW, but a negative correlation was found in TWW (Table 2). This relationship was different for every area as shown the statistical comparison of intercepts and slopes of regression equations (*t*-student, $\alpha = 0.05$). Chl *a* concentration accounted for 29% of the variance in the abundance of heterotrophic bacteria for the whole area of study (Table 2).

Bacterial subpopulations: HNA and LNA

The Antarctic heterotrophic bacterial community from 0 to 100 m showed at least two bacterial subpopulations in all samples analysed that were similar to the HNA and LNA subpopulations found in different aquatic environments (Fig. 3). These subpopulations were clearly distinguishable in a bivariate plot of green fluorescence against wide angle light scatter. A third subpopulation, apparently derived from HNA, was observed in some samples (results not shown), however, we did not analyse this third subpopulation independently because it appeared only occasionally. Although HNA and LNA subpopulations showed differences in SSC, the main difference between them were found in the mean level of FL1, that is, the apparent content of nucleic acids per cell (Fig. 3). HNA and LNA subpopulations differed considerably in their response to several environmental variables: (1) The mean intensity of green fluorescence for the HNA fraction (FL1-HNA), that is, the mean apparent content of nucleic acid per cell for the HNA subpopulation, decreased with depth while the mean fluorescence signal of the LNA subpopulation (FL1-LNA) remained constant (Fig. 3). (2) The mean apparent content of nucleic acids per cell in the HNA subpopulation increased significantly with Chl *a* concentration, while the mean apparent content of nucleic acids per cell for LNA remained constant for a wide range of Chl *a* concentrations (Fig. 4a, Table 3). The relative contribution of both fractions to the total bacterial population changed considerably among samples. The percentage of HNA cells (%HNA) ranged between 35.0 and 76.7 ($62.2 \pm 8.1\%$). FL1-HNA was significantly correlated with Chl *a*, but we did not find a significant correlation between %HNA and Chl *a* (Fig. 4b).

Apparent content of nucleic acids

The apparent content of nucleic acids per cell for the HNA subpopulation, estimated by the relative intensity of green fluorescence changed with depth (Fig. 3). FL1-HNA tended to decrease with depth for the whole area of study and when data from each hydrographic zone were analysed separately (Fig. 5). The mean vertical pattern of FL1-HNA presented a subsurface maximum at 10 m that was very clear in Gerlache and Bransfield Straits and less evident in Drake Passage. For all stations, the mean values of FL1-HNA in surface (5 m) and at 100 m were 96 and 79%, respectively, of that found at the maximum. Mean vertical profiles of the apparent nucleic acid content for each zone were similar to the mean Chl *a* profiles. This explains the significant corre-

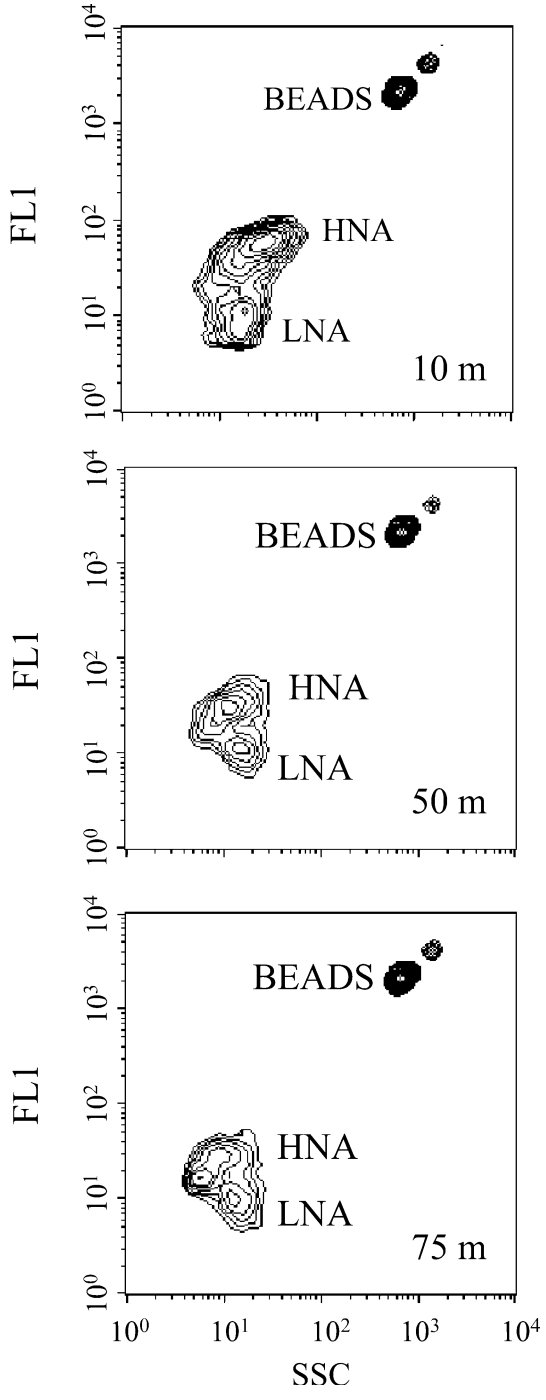

Fig. 3 Representative bivariate plot of SYTO 13-induced green fluorescence intensity per cell (apparent content of nucleic acids) against 90°-side scatter (SSC) for three different depths at station G1 in Gerlache Strait. Note the variation in the position of the peaks

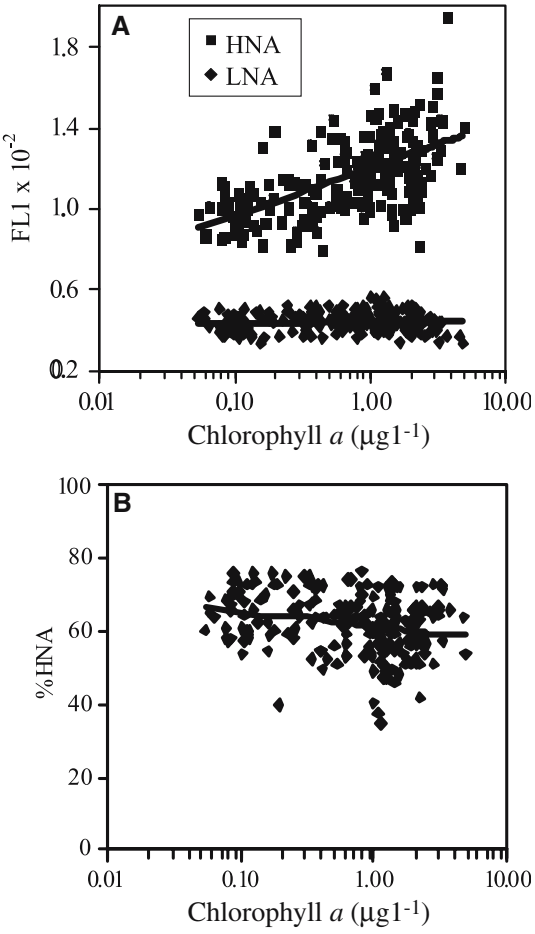

Fig. 4 **a** Relationship between SYTO 13-induced green fluorescence intensity per cell (arbitrary units), for HNA (FL1-HNA) and LNA (FL1-LNA), and chlorophyll a concentration for the whole study area. Regression equations were Log FL1-HNA = −1.955 + 0.088 Log Chl *a* (r^2 = 0.363) and Log FL1-LNA = −2.355 + 0.003 Log Chl *a* (r^2 = 0.001), respectively (see Table 3 for details). **b** Relationship between the percentage of the HNA subpopulation of total heterotrophic bacteria (%HNA) and Chl *a*

lation found between FL1-HNA and Chl *a* for all stations (Fig. 4), and suggests a close relationship between apparent nucleic acid content for the active fraction of the bacterial population and standing stock of autotrophic biomass. On the contrary, FL1-LNA did not change either with depth or with Chl *a* concentration (Figs. 3, 4).

Wide angle light scatter

We found marked differences among HNA and LNA subpopulations regarding the way in which their wide angle light scatter signals changed with depth. These differences were apparent either when a single station was analysed or when the whole data set were considered. The SSC signal of the HNA subpopulation (SSC-HNA) decreased with depth. However, SSC of the LNA subpopulation (SSC-LNA) remained almost constant with depth (Fig. 6). These vertical patterns in the changes of SSC for HNA and LNA subpopulations did not change when data for all stations were pooled together despite horizontal heterogeneity in both autotrophic and heterotrophic microbial biomass (Fig. 7). Changes in depth accounted for 46% in the variability of the mean SSC-HNA, but only 7.8% of SSC-LNA (Fig. 7a, Table 3). Mean SSC signals from HNA and LNA subpopulations differed in their response to increasing levels of Chl *a*.

Table 3 Linear regressions between several variables for the whole available data set (35 stations). Standard errors (SE) of the intercepts and slopes are shown in brackets. Determination coefficient (r^2), number of samples (n), and p-value (p) are shown as well

Dependent variable	Intercept (SE)	Slope (SE)	Independent variable	r^2	n	p
Log THB	5.533(0.009)	0.163(0.017)	Log Chl *a*	0.290	222	< 0.01
Log FL1-HNA	−.925(0.004)	0.088(0.008)	Log Chl *a*	0.363	216	< 0.01
Log FL1-LNA	−.355(0.003)	0.003(0.006)	Log Chl *a*	0.001	216	0.230
%HNA	63.684(0.839)	−.393(0.598)	Chl *a*	0.024	217	0.024
Log SSC-HNA	−.762(0.005)	0.142(0.010)	Log Chl *a*	0.473	216	< 0.01
Log SSC-LNA	−.570(0.002)	0.016(0.005)	Log Chl *a*	0.049	216	< 0.01
Log SSC-HNA	−.702(0.008)	−.002(0.0001)	Depth (m)	0.460	216	< 0.01
Log SSC-LNA	−.570(0.03)	−.0003(0.00007)	Depth (m)	0.078	216	< 0.01
%HNA	17.955(6.197)	1.603(0.222)	Nitrate	0.207	200	< 0.01
%HNA	24.791(7.711)	17.129(3.502)	Phosphate	0.109	200	< 0.01

THB total heterotrophic bacteria, *FL1-HNA* apparent nucleic acid content of the HNA subpopulation, *FL1-LNA* apparent nucleic acid content of the LNA subpopulation, *SSC-HNA* side scatter level of HNA and LNA *SSC-LNA*, *%HNA* percentage of HNA bacteria

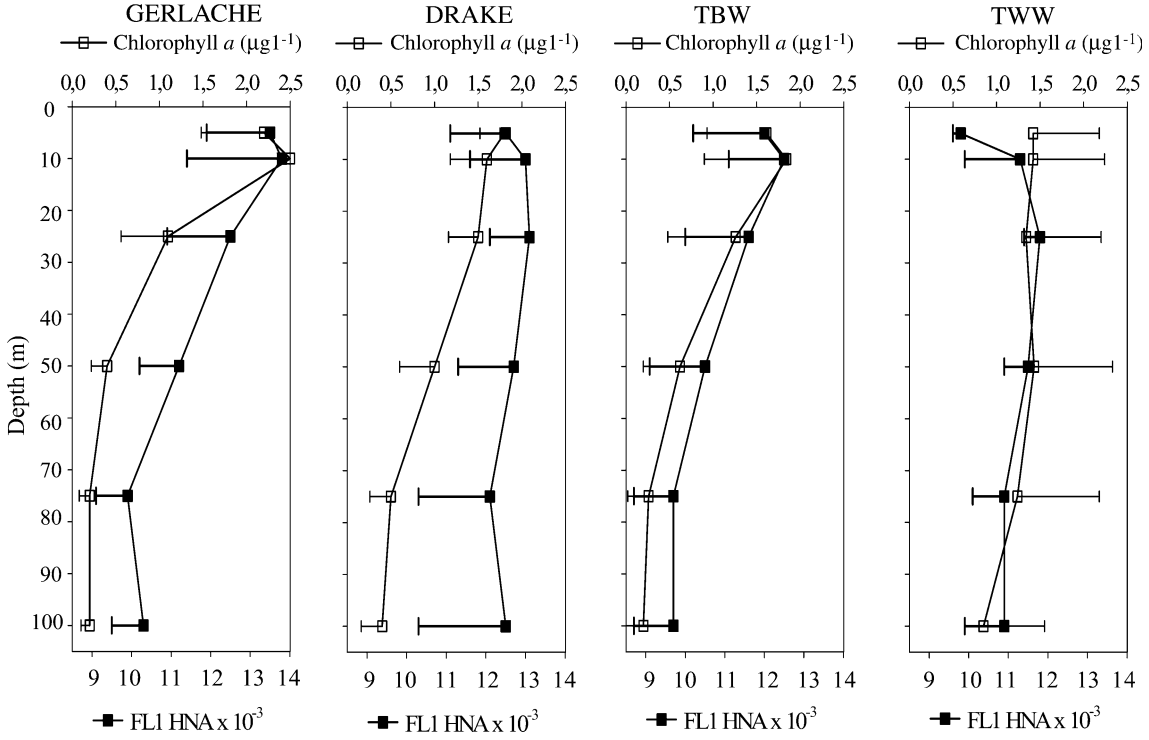

Fig. 5 Vertical profiles of Chl *a* and green fluorescence intensity per cell, in arbitrary units, for the HNA (FL1-HNA) in the four zones. Represented data are the average and the SD values have been plotted as a single arm bar for clarity sake. Transitional Zonal Water with Bellingshausen Sea influence (TBW), Transitional Zonal Water with Weddell Sea influence (TWW)

Mean SSC-HNA showed a strong positively correlation with Chl *a* concentration, which accounted for about 47% of variability in mean SSC-HNA (Fig. 7b, Table 3). However, Chl *a* only accounted for about 5% of variability in mean SSC-LNA (Table 3).

Vertical pattern of %HNA

The percentage of heterotrophic bacteria with high apparent nucleic acid content per cell changed with depth. Maximum increase in %HNA was observed between 5 and 10 m. Mean %HNA for all stations increased significantly from 58 ±8.2% at surface to 65 ± 6.2% at 100 m ($n = 35$, $P < 0.01$). This general pattern was also found when each hydrographic zone was analysed separately, although the vertical profiles of %HNA in Drake Passage and TWW were more homogeneous (Fig. 8). Mean %HNA (Table 1) for every oceanographic area were statistically different (t-student, $\alpha = 0.05$). The vertical profiles of %HNA were inverse to those of Chl *a* concentration, total bacterial abundances and apparent nucleic acid content (Figs. 2, 5). No significant correlation was found between Chl *a* concentration and %HNA (Fig. 4b). %HNA tended to covariate with potential density (Fig. 9) and variables directly influenced by the water column stratification like the concentrations of nitrate

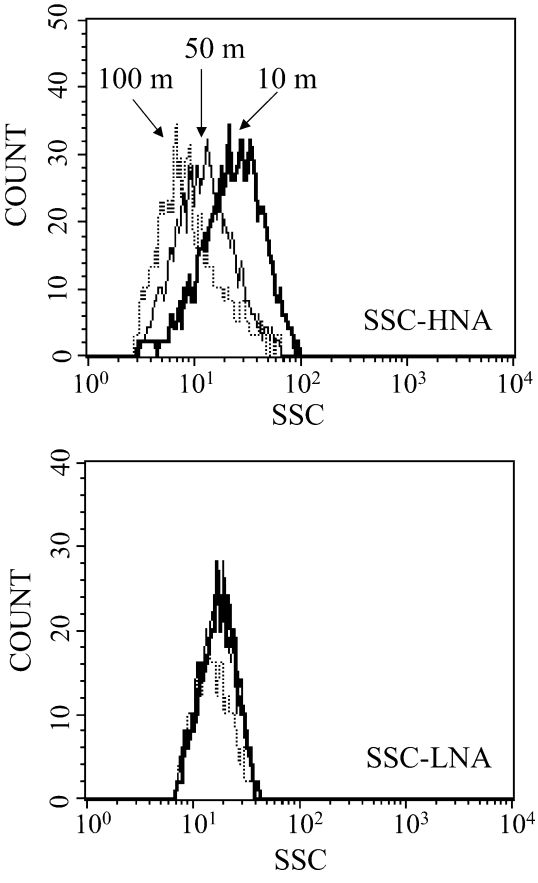

Fig. 6 Representative histograms of SSC for the HNA and the LNA bacterial subpopulations at three depths (10, 50 and 100 m) for station G1. Data are expressed as number of cells (counts) in each of the 1024 channel in which the intensity of the SSC signal is classified by the flow cytometer data-processing software

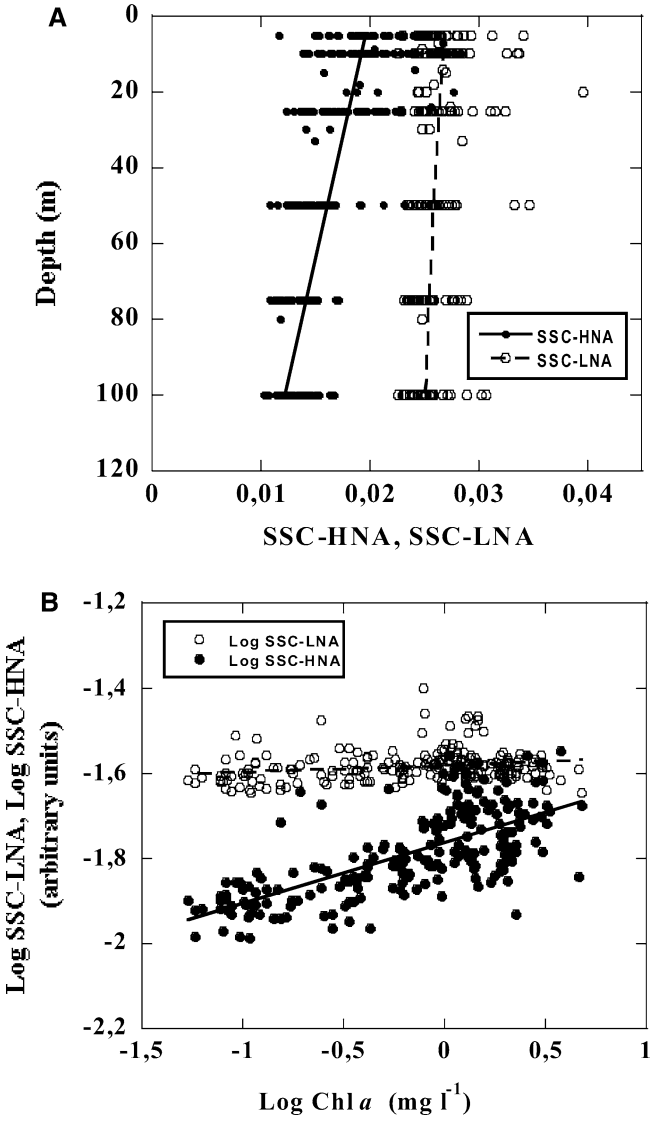

Fig. 7 Relationship between mean SSC signal for the HNA (SSC-HNA) and for the LNA subpopulations (SSC-LNA) with depth **A** and with Chl *a* concentration **B** for the whole study area

and phosphate in the water column (Table 3). The apparent relationship between %HNA and potential density was specific of each area or water mass because the statistical comparison of intercepts and slopes of the regression equations showed that they were significantly different (*t*-student, $\alpha = 0.05$).

Discussion

Autotrophic biomass and total bacterial abundance

Both chlorophyll concentration and abundance of heterotrophic bacteria were in the same range as those reported by Holm-Hansen and Mitchell (1991) and Karl et al. (1991) during the RACER cruise and those of Varela et al. (2002) and Pedrós-Alió et al. (2002) for the FRUELA cruises in basically the same area. This concordance in the abundance of heterotrophic bacteria encompasses studies done during the last 13 years and using two different methodologies: epifluorescence microscopy (Karl et al. 1991; Pedrós-Alió et al. 2002) and flow cytometry (this study). This area is hydrographically complex, supporting horizontal and vertical distributions of Chl *a* largely heterogeneous (Lipski 1985; Schloss and Estrada 1994; Figueiras et al. 1998; Basterretxea and Arístegui 1999; Corzo et al. 2005). The variability in abundance of total bacteria was lower (Table 1). Total bacterial biomass tends to be less variable than the autotrophic component of the planktonic community (Cole and Caraco 1993; del Giorgio and Gasol 1995).

Abundance of total heterotrophic bacteria was significantly correlated with Chl *a* level when the whole data set was analysed or when it was divided by zones. In all cases the correlation between Bacteria and Chl *a* was positive, except in the two stations showing characteristics of TWW (Table 2). The different regression equations were significantly different and this is a further confirmation of the high heterogeneity of this region. The slope of the regression between heterotrophic bac-

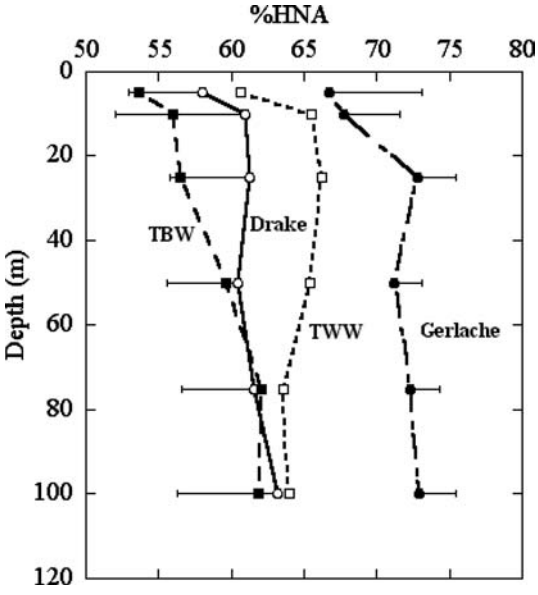

Fig. 8 Average vertical profiles of the percentage of HNA subpopulation to total bacteria population (%HNA) for Drake Passage, Gerlache and Bransfield Straits. Standard deviations for all profiles ranged between 0.72 and 8.99, they are shown as a single arm bar only for Gerlache and Drake for clarity. TBW and TWW average data showed similar SD, Transitional Zonal Water with Bellingshausen Sea influence (TBW), Transitional Zonal Water with Weddell Sea influence (TWW)

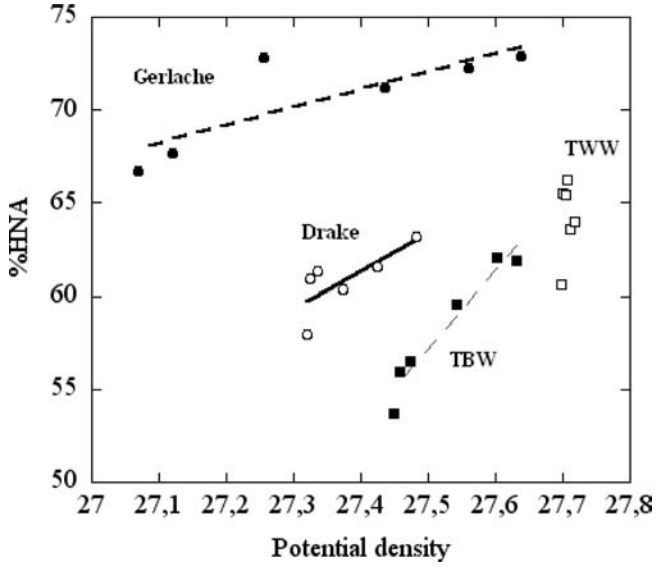

Fig. 9 Relationship between %HNA and potential density for Drake Passage, Gerlache and Bransfield Straits. Transitional Zonal Water with Bellingshausen Sea influence (TBW), Transitional Zonal Water with Weddell Sea influence (TWW). Regression equations of lines shown are: $y = -90{,}80 + 9.56x$, $r^2 = 0.676$ (Gerlache), $y = -93.12 + 20.24x$, $r^2 = 0.592$ (Drake), $y = -111.40 + 59.87x$, $r^2 = 0.936$ (TBW)

teria and Chl *a* found for different pelagic environments and in across-systems comparisons can be interpreted in a trophodynamic sense (Bird and Kalff 1984; Cole et al. 1988; Pedrós-Alió et al. 2000). The slope calculated by us was lower than those of available general relationships including data for different systems (Cole et al. 1988; Pedrós-Alió et al. 2000). This apparent inefficient transfer of C between primary producers and heterotrophic bacteria seems to be a characteristic feature of this area since it was also observed during RACER and FRUELA (Karl et al. 1991; Pedrós-Alió et al. 2002). Both bottom-up and top-down causes, including viral lysis, have been suggested to control the abundance of heterotrophic prokaryotes in the Southern Ocean (Boyd et al. 2000; Moran and Estrada 2002; Pedrós-Alió et al. 2002; Vaqué et al. 2002). Little information exists on how these factors might affect the proportion of active bacteria and their activity level in situ.

Apparent nucleic acid content: HNA and LNA subpopulations

The analysis of heterotrophic bacterioplankton by flow cytometry in the Antarctic waters revealed the presence of several subpopulations that differed in the degree of SYTO 13 staining and, therefore, in their apparent cell content of nucleic acids (Fig. 3). In most samples we found only two well-discriminated subpopulations (LNA and HNA), although in some cases we detected a third subpopulation apparently derived from HNA. Occasionally, three bacterial subpopulations have been found in marine samples (Li et al. 1995; Marie et al. 1997) and in lakes where the third subpopulation was interpreted as large cells growing at a rate fast enough to contain replicated DNA (Button et al. 1996). The presence of several subpopulations differing in their apparent content of nucleic acid is a characteristic of free pelagic bacterial communities. They have been found, using different dyes, in all aquatic media so far investigated (Gasol and del Giorgio 2000) including Antarctic waters (this study). However, the ecological significance of these subpopulations is unknown, although there is strong evidence that they represent bacterial assemblages differing in the level of metabolic activity (Li et al. 1995; Servais et al. 1999; Gasol and del Giorgio 2000; Lebaron et al. 2001; Servais et al. 2003). Bacteria with very low metabolic activity, resting cells, dead cells, fragments of cells, large viruses and even large free DNA fragments have been suggested to integrate the LNA population (Zweifel and Hagström 1995; Jellett et al. 1996; Choi et al. 1996; Heissenberger et al. 1996; Gasol et al. 1999), but also small active cells (Zubkov et al 2001). However recently, cell sorting and molecular biology techniques suggest that LNA and HNA cells are not phylogenetically different bacteria (Servais et al. 2003; Longnecker et al. 2005). They are more likely the cells with different apparent content of nucleic acid and with different cell-specific activity (Servais et al. 2003). LNA subpopulation appeared in the culture of marine bacteria only in the stationary growth phase (Lebaron et al. 2002). However, it seems

that LNA cells are not fully inactive (Longnecker et al. 2005).

The HNA and LNA fractions of bacterial community differed largely in the apparent content of nucleic acid per cell. Likely, most of the difference in fluorescence intensity detected after SYTO 13 staining among individual bacteria is related to changes in RNA content, particularly ribosomal RNA (rRNA). Two lines of evidence support our interpretation: (1) SYTO 13 stained both DNA and RNA and their contribution to the total fluorescence per cell changed with growth rate (Guindulain et al. 1997; Troussellier et al. 1999; Guindulain and Vives-Rego 2002). (2) The cell content of RNA is much higher than DNA, specially rRNA changes considerably during cell cycle and with growth rate (Maaløe and Kjeldgaard 1966; Kemp et al. 1993; Kramer and Singleton 1993; Karner and Fuhrman 1997).

The heterotrophic bacterial community in any natural sample is formed by many different species with different genome sizes. In Antarctic waters, in addition to *Bacteria, Archaea* are known to comprise a significant fraction of the picoplankton community (DeLong et al. 1994; Massana et al. 1998; Murray et al. 1998). Staining of cells with SYTO 13 and their analysis by flow cytometry cannot discriminate within this taxonomic diversity because only two or, some time, three different subpopulations appeared. It is possible that changes in rRNA content, closely related to growth stage, overrides changes in DNA content due to taxonomic differences.

Differences in the response of HNA and LNA subpopulations to environmental factors in situ

LNA and HNA subpopulations differed in the way in which their apparent content of nucleic acid changed with environmental factors. HNA bacteria were a more dynamic component of the total bacterial community, their fluorescence intensity per cell decreased with depth and showed a vertical pattern similar to that of autotrophic biomass (Figs. 3, 5). This covariation between FL1-HNA and Chl *a* and the difference regarding FL1-LNA versus Chl *a* were also observed pooling all data (Fig. 4a). These observations for Antarctic bacterioplankton are similar to those reported in the only two previous studies, as far as we know, dealing with changes in the abundances and flow cytometer signatures of HNA and LNA subpopulations in marine ecosystems (Li et al. 1995; Jellet et al. 1996). Both studies were done at lower latitudes. In both cases the apparent content of nucleic acid per cell for the HNA subpopulation was positively correlated with the standing stock of Chl *a* and decreased with depth. No similar trends were observed for the LNA subpopulation (Li et al. 1995; Jellet et al. 1996). However, a major difference between the Antarctic and lower latitudes was that in both studies the %HNA was also correlated with standing stocks of Chl *a*. An additional difference is that %HNA decreased with depth in Bedford Basin (Jellet et al. 1996). On the contrary, %HNA increased with depth in Antarctic waters, although there were differences among zones (Fig. 8), and we did not find a significant correlation between %HNA and Chl *a* (Fig 4b). It is not clear what causes these differences. In principle, %HNA should covariate with mean metabolic activity and growth rate for the whole bacterial population because more bacteria would be metabolically active and therefore dividing, this being the rationale of the so-called active cell index (Li et al. 1995; Jellet et al. 1996). However, differences in the standing stocks of the HNA cells could neither reflect differences in their growth rate nor metabolic activity if we compare populations under distinct turnover rates. A low %HNA could be compatible with a high turnover rate of the HNA population if this fraction is under a high grazing pressure or a high viral lysis rate.

The empirical evidence from laboratory and microcosms experiments (Gasol et al. 1999; Servais et al. 1999; Lebaron et al. 2001) and field studies (Li et al. 1995; Jellet et al. 1996; Servais et al. 2003) suggests that HNA cells are more active and dynamic than LNA cells and they were responsible of most of total bacterial production. Even in the same sample, the HNA subpopulation was not integrated by identical cells and showed a higher degree of heterogeneity than the LNA subpopulation both in the intensity of green fluorescence and in SSC (Figs. 3, 6). Cell-specific rates of leucine incorporation and growth rate were positively correlated with both the nucleic acid content of cells and their SSC signal (Lebaron et al. 2002). Particularly interesting for the analysis of the ecological significance of both subpopulations is that LNA cells were not detected in the log growth phase, but they were present in the stationary phase (Lebaron et al. 2002). Therefore, the vertical profiles of FL1-HNA and their horizontal variation might be interpreted as a proxy of changes in metabolic activity and growth rate of the active fraction of Antarctic bacterioplankton.

Wide angle light scatter of the HNA and LNA subpopulations

Changes in bacterial size can be estimated from changes in the SSC signal (Servais et al 1999; Bernard et al. 2000; Lebaron et al. 2002; Servais et al. 2003). SSC provides a better measure of the relative cell size for organisms in the picoplanktonic range because of its higher sensitivity to small changes as compared to forward light scatter (Dubelaar and Jonker 2000; Jochem 2000).

The SSC signals (apparent cell sizes) of HNA and LNA cells seem to be under different environmental control. Observed variability in apparent cell size was larger in HNA than in LNA bacteria as revealed by a simple comparison of their coefficients of variation (24 and 9%, respectively). The apparent cell size of the HNA population increased with Chl *a* concentration and decreased with depth. Both trends are likely to be

related due to the inverse relationship between Chl *a* and depth. Both environmental factors explained about 46% of the observed variability in apparent cell size of the HNA bacteria (Table 3). On the contrary, the apparent cell size of the LNA fraction did not change significantly neither with Chl a nor with depth (Figs. 6, 7).

Cell size of heterotrophic bacteria is linearly correlated with growth rate (Maaløe and Kjeldgaard 1966; Davey and Kell 1996). The little information available for marine bacterial communities suggests that a similar relationship exists between biovolume, estimated from the SSC signal, and growth rate at least for the low range of sizes (Servais et al. 1999; Bernard et al. 2000). In addition, cell size was also positively related to bacterial production and the apparent content of nucleic acid for the HNA subpopulation (Lebaron et al. 2002).

The simplest interpretation for the observed patterns of changes in apparent cell size of the HNA and LNA bacteria is the following. Active heterotrophic bacteria, the HNA fraction, were bigger and likely grew faster close to the surface where primary production supplied more organic carbon for growth. They were smaller and likely growing at a lower rate as depth increased. A variable fraction of the total bacterial community remained in a less active or inactive state showing little or no change at all with Chl *a* or depth.

Top-down and bottom-up mechanisms affecting HNA and LNA subpopulations

The percentage of active bacteria increased with depth in Antarctic waters (Fig. 8). This increase cannot be interpreted as an indication of higher relative metabolic activity and growth rate as depth increases because vertical distributions of phytoplankton and bacterial production are related and decrease with depth. Therefore, it seems that the active cell index (Jellet et al. 1996) cannot be properly applied to Antarctic waters. It is unclear what caused the observed vertical pattern in %HNA, but the vertical distribution of grazing in the water column might play a role. Grazing rate by heterotrophic nanoflagellates and other planktonic grazers seems to be size dependent, cropping selectively the biggest and more active fraction of bacterioplankton (Andersson et al. 1986; Sherr and Sherr 1994; Gasol et al. 1995; del Giorgio et al. 1996b). Grazers will crop selectively the HNA population reducing its contribution to total bacteria because it is likely that the grazing activity will be coincident in space with bacterial production, mainly supported by the HNA fraction. This could explain the observed increase in %HNA with depth. Available information from Antarctica and other marine areas supports our hypothesis. Both grazer abundance and virus abundance in the area show vertical profiles that could explain those of %HNA (Guixa-Boixereu et al. 2002; Vaqué et al. 2002), but more experimental work is needed to address specifically how grazing could affect the vertical and horizontal distribution of %HNA in different oceanographic conditions. Similar patterns in the vertical distribution of %HNA were observed in the Gulf of Mexico (Jochem 2001, 2004).

HNA cells are not identical regarding the intensity of SYTO 13-induced fluorescence per cell, and although %HNA was lower in surface our results show that the mean apparent content of nucleic acids changed with depth, following a pattern similar to that of Chl *a* concentration. Mean FL1-HNA was maximum at 10 m where Chl *a* peaked as well. This means that HNA bacteria, accounted for a lower fraction of the total bacterial community, but were more active and bigger in the surface, close to the Chl *a* maximum, than at higher depth. The availability of fresh dissolved organic carbon would determine the level of metabolic activity within this fraction. This is likely why FL1-HNA presented a vertical profile similar to that of standing stock of Chl *a*.

Obviously, the stability of the water column is determinant for the vertical distribution of inorganic nutrients, autotrophic biomass, and bacterioplankton and its predators. Likely, the more homogeneous profiles of %HNA in Drake Passage and TWW are related to higher degree of uniformity in the vertical profile of potential density. On the contrary, stronger stratification in Gerlache Strait and TBW seems to sustain more heterogeneity in the vertical distribution of %HNA. Other unresolved questions that should be addressed are why the mean %HNA and its relationship with potential density for distinct zones or water masses are different. Differences in the abundance of phytoplankton could explain part of the observed variability, but in Gerlache Strait, maximum mean value of %HNA coincided with the minimum mean value of integrated chlorophyll (Table 1). Differences in grazing pressure between water masses could also contribute to explain the observed differences in mean %HNA.

Conclusions

The analysis by flow cytometry of Antarctic bacterioplankton shows the existence of two subpopulations of cells, LNA and HNA, that differed markedly in their response to changes in several ecological factors. Our field results agree with the identification of the HNA subpopulation with the active fraction of the heterotrophic bacterial community in Antarctic waters. We have shown here that apparent content of nucleic acid is a sensitive variable that responded to changes in depth, water column stability and autotrophic biomass in a consistent way. Several authors have shown that the apparent content of nucleic acid is related to the activity and growth rate of bacterial cell. Taking together both lines of evidences we suggest that the analysis of changes in space and time of this variable in the ocean could provide a valuable tool to increase our knowledge on bacterioplankton ecology. Changes in FL1-HNA and SSC-HNA represent the response to environmental

factors at an individual level, while variations in the relative abundances of the HNA and LNA fractions and total bacteria represent the response at a population and/or community level. Surprisingly, %HNA tended to increase with depth. At the moment, it is unclear what causes this pattern in Antarctic waters and even what happens elsewhere. It is important to notice that the vertical distribution of %HNA was opposite to expected distributions of primary producers and bacterial production. The increase of %HNA with depth could result from a higher grazing pressure close to the surface, where the most active and largest cells occurred. As in many other biological properties, the degree of stratification plays a role in the shape of the vertical distribution of %HNA. Relatively, homogeneous profiles were observed in areas with low vertical differences in potential density, while larger increases of %HNA with depth occurred when the stability of the water column was higher due to vertical differences in potential density.

Acknowledgments This work was financially supported by grants MAT2000-0261-P4-04, REN2002-01281/MAR, and REN2001-2650/ANT from the Ministerio de Ciencia y Tecnología, Spain. We acknowledge the support and help of the Officers and Crew of BIO-Hespérides during cruise CIEMAR. Authors thanks Pep Gasol, Carles Pedrós-Alió and several anonymous referees for their time, comments and suggestions.

References

Andersson A, Larsson U, Hagström A (1986) Size-selective grazing by a microfagellate on pelagic bacteria. Mar Ecol Progr Ser 33:51–57

Basterretxea G, Arístegui J (1999) Pytoplankton biomass and production during late austral spring (1991) and summer (1993) in the Bransfield Strait. Polar Biol 21:11–22

Bernard L, Courties C, Servais P, Trousellier M, Petit M, Lebaron P (2000). Relationships among bacterial cell size, productivity, and genetic diversity in aquatic environments using cell sorting and flow cytometry. Microb Ecol 40:148–158

Bird DF, Kalff J (1984) Empirical relationship between bacterial abundance and chlorophyll concentration in fresh and marine waters. Can J Fish Aquat Sci 41:1015–1023

Boyd P and others (2000) A mesoscale phytoplankton bloom in the polar Southern Ocean stimulated by iron fertilization. Nature 407:695–702

Button DK, Robertson BR, Jüttnerf (1996) Microflora of a subalpine lake: bacterial populations, size and DNA distributions, and their dependence on phosphate. FEMS Microbiol Ecol 21:87–101

Choi JW, Sherr EB, Sherr BF (1996) Relation between presence-absence of a visible nucleoid and metabolic activity in bacterioplankton cells. Limnol Oceanogr 41:1161–1168

Cole JJ, Findlay S, Pace ML (1988) Bacterial production in fresh and saltwater ecosystems: a cross-systems overview. Mar Ecol Prog Ser 43:1–10

Cole JJ, Caraco NF (1993) The pelagic microbial food web of oligotrophic lakes, pp. 101–112. In: T. Ford (ed) Aquatic microbiology, Blackwell Scientific Press

Corzo A, Rodríguez-Gálvez S, Lubian L, Sangrá P, Martínez A, Morillo JA (2005) Spatial distribution of transparent exopolymer particles (TEP) in the Bransfield Strait (Antarctica). J Plank Res (in press)

Davey HM, Kell DB (1996) Flow cytometry and cell sorting of heterogeneous microbial populations: the importance of single-cell analysis. Microbiol Rev 60:641–696

DeLong EF, Wu KY, Prezelin BB, Jovine RVM (1994) High abundance of archaea in Antractic marine picoplankton. Nature 371:695–697

del Giorgio P, Gasol JM (1995) Biomass distribution in freshwater plankton communities. Am Nat 146:135–152

del Giorgio PA, Bird DF, Prairie YT, Planas D (1996a) Flow cytometric determination of bacterial abundance in lake plankton with the green nucleid acid stain SYTO 13. Limnol Oceanogr 41:783–789

del Giorgio PA, Gasol JM, Vaqué D, Mura P, Agustí S, Duarte CM (1996b) Bacterioplankton community structure: protists control net production and the proportion of active bacteria in a coastal marine community. Limnol Oceanogr 41:1169–1179

Dubelaar GBJ, Jonker BR (2000) Flow cytometry as a tool for the study of phytoplankton. Sci Mar 64:135–156

Figueiras FG, Estrada M, López O, Arbones B (1998). Photosynthetic parameters and primary production in the Bransfield Strait: relationships with mesoscale hydrographic structures. J Mar Systems 17:129–141

García MA, Castro CG, Ríos AF, Doval MD, Rosón G, Gomis D, López O (2002) Water masses and the distribution of physico-chemical properties in the Western Bransfield Strait and Gerlache Strait during austral summer 1995/96. Deep-Sea Res II 49:585–602

Gasol JM, del Giorgio PA (2000) Using flow cytometry for counting natural planktonic bacteria and understanding the structure of planktonic bacterial communities. Sci Mar 64:197–224

Gasol JM, del Giorgio PA, Massana R, Duarte CM (1995) Active versus inactive bacteria: size-dependence in a coastal marine plankton community. Mar Ecol Prog Ser 128:91–97

Gasol JM, Zweifel UL, Peters F, Fuhrman JA, Hagström A (1999) Significance of size and nucleic acid content heterogeneity as measured by flow cytometry in natural plaktonic bacteria. Appl Environ Microbiol 65:4475–4483

Grasshoff K, Ehrhardt M, Kremling K (1983) Methods of sea water analysis. Verlag Chemie

Guindulain T, Comas J, Vives-Rego J (1997) Use of nucleic acid dyes SYTO-13, TOTO-1, and YOYO-1 in the study of *Escherichia coli* and marine prokaryotic populations by flow cytometry. Appl Environ Microbiol 63:4608–4611

Guindulain T, Vives-Rego J (2002) Involvement of RNA and DNA in the stainig of *Escherichia coli* by SYTO 13. Lett Appl Microbiol 34:1–7

Guixa-Boixereu N, Vaqué D, Gasol JM, Sánchez-Camara J, Pedrós-Alió C. Viral distribution and activity in Antarctic waters. Deep-Sea Res II 49:827–846

Heissenberger A, Leppard GG, Herndl GJ (1996) Relationship between the intracellular integrity and the morphology of the capsular envelope in attached and free-living marine bacteria. Appl Environ Microbiol 62:4521–4528

Holm-Hansen O, Lorenzen C J, Holmes RW, Stickland JDH (1965) Fluorimetric determination of chlorophyll. J Cons Perm Int Explo Mer 30:3–15

Holm-Hansen O, Mitchell BG (1991) Spatial and temporal distribution of phytoplankton and primary production in the western Bransfield strait region. Deep-Sea Res 38:961–980

Jacquet S, Lennon JF, Marie D, Vaulot D (1998) Picoplankton population dynamics in coastal waters of the northwestern Mediterranean Sea. Limnol Oceanogr 43:1916–1931

Jellet JF, Li WKW, Dickie PM, Boraie A, Kepkay PE (1996) Metabolic activity of bacterioplankton communities assed by flow cytometry and single carbon substrate utilization. Mar Ecol Prog Ser 136:213–225

Jochem FJ (2000) Probing the physiological state of phytoplankton at the single-cell level. Sci Mar 64:117–268

Jochem FJ (2001) Morphology and DNA content of bacterioplankton in the northern Gulf of Mexico: analysis by epifluorescence microscopy and flow cytometry. Aquat Microb Ecol 25:179–194

Jochem FJ, Lavrentyev PJ, First MR (2004) Growth and grazing rates of bacteria groups with different apparent DNA content in the Gulf of Mexico. Mar Biol 145:1213–1225

Jürgens K, Güde H (1994) The potential importance of grazing-resistant bacteria in planktonic systems. Mar Ecol Prog Ser 112:169–188

Karl DM, Holm-Hansen O, Taylor GT, Tien G, Bird DF (1991) Microbial biomass and productivity in the Western Bransfield Strait Antarctica during 1986–87 Austral winter. Deep-Sea Res II 38:1029–1055

Kemp PF, Lee S, LaRoche J (1993) Estimating the growth rate of slowly growing marine bacteria from RNA content. Appl Environ Microbiol 59:2594–2601

Karner M, Fuhrman JA (1997) Determination of active marine bacterioplakton: a comparison of universal 16S rRNA probes, autoradiography, and nucleoid stainig. Appl Environ Microbiol 63:1208–1213

Kramer J, Singleton FL (1993) Measurement of rRNA variations in natural communities of microorganisms in the southeastern U.S. continental shelf. Appl Environ Microbiol 59:2430–2436

Lebaron P, Servais P, Agogué H, Courties C, Joux F (2001). Does the high nucleic acid content of individual bacterial cells allow us to discriminate between active cells and inactive cells in aquatic systems? Appl Environ Microbiol 67:1775–1782

Lebaron P, Servais P, Baudoux AC, Bourrain M, Curties C, Parthuisot N (2002). Variations of bacterial-specific activity with cell size and nucleic acid content assessed by flow cytometry. Aquat Microb Ecol 28:131–140

Li WKW, Jellet JF, Dikie PM (1995) DNA distributions in planktonic bacteria stained with TOTO or TO-PRO. Limnol Oceanogr 40:1485–1495

Lipski M (1985) Chlorophyll a in the Bransfield Strait and the southern part of Drake Passage during BIOMASS_SIBEX (December 1983–January 1984). Pol Polar Res 6:21–30

Longnecker K, Sherr BF, Sherr EB (2005) Activity and phylogenetic diversity of high and low nucleic acid content, ETS-active, bacterial cells in an upwelling ecosystem. Apply Envirom Microb (submitted)

Maaløe O, Kjeldgaard NO (1966) Control of macromolecular synthesis. A study of DNA, RNA and protein synthesis in bacteria. W.A. Benjamin, Inc.

Marie D, Partensky F, Jacquet S, Vaulot D (1997) Enumeration and cell cycle análisis of natural populations of marine picoplankton by flow cytometry using the nucleic acid stain SyberGreen I. Appl Environ Microbiol 63:186–193

Massana R, Taylor LT, Murray AE, Wu KY, Jeffrey WH, DeLong EF (1998) Vertical distribution and temporal variation of marine planktonic archaea in the Gerlache Strait, Antarctica, during early spring. Limnol Oceanogr 43:607–617

Moran XAG, Estrada M (2002) Pytoplanktonic DOC and POC production in the Bransfield and Gerlache Straits as derived from kinetic experiments of 14C incorporation. Deep-Sea Res II 49:769–786

Monfort P, Baleux B (1992) Comparison of flow cytometry and epifluorescence microscopy for counting bacteria in aquatic ecosystems. Cytometry 13:188–192

Monger BC, Landry MR (1993) Flow cytometry analysis of some marine bacteria with Hoechst 33342. Mar Eol Prog Ser 59:905–911

Murray AE, Preston CM, Massana R, Taylor LT, Blakis A, Wu K, DeLong EF (1998) Seasonal and spatial variability of bacterial and archaeal assemblages in the coastal waters near Anvers Island, Antarctica. Appl Environ Microbiol 64:2585–2595

Pedrós-Alió C, Calderón-Paz JI, Gasol JM (2000) Comparative analysis shows that bacterivory, not viral lysis, controls the abundance of heterotrophic prokaryotic plankton. FEMS Microbiol Ecol 32:157–165

Pedrós-Alió C, Vaqué D, Guixa-Boixereu N, Gasol JM (2002) Prokaryotic plankton biomass and heterotrophic production in western Antartic waters during 1995–1996 Austral Summer. Deep-Sea Res II 49:805–825

Robertson BK, Button DK (1989) Characterizing aquatic bacteria according to population, cell size and apparent DNA content by flow cytometry. Cytometry 10:70–76

Rodríguez J, Jiménez-Gómez F, Blanco JM, Figueroa FL (2002) Physical gradients and spatial variability of the size structure and composition of phytoplankton in the Gerlache Strait (Antarctica). Deep-Sea Res II 49:693–706

Schloss I, Estrada M (1994) Phytoplankton composition in the Weddell-Scotia confluence area during austral spring in relation to hydrography. Polar Biol 14:77–90

Servais P, Courties C, Lebaron P, Troussellier M (1999) Coupling bacterial activity measurements with cell sorting by flow cytometry. Microb Ecol 38:180–189

Servais P, Casamayor EO, Courties C, Catala P, Partuisot N, Lebaron P (2003) Activity and diversity of bacterial cells with high and low nucleic acid content. Aquat Microb Ecol 33:41–51

Sherr, BF, Sherr, EB, McDaniel, J (1992). Effect of protistan grazing on the frequency of dividing cells (FDC) in bacterioplankton assemblages. Appl Environ Microbiol 58:2381–2385

Sherr EB, Sherr BF (1994) Bacterivory and herbivory: Key roles of phagotrophic protists in pelagic food webs. Microb Ecol 28:127–133

Troussellier M, Courties C, Lebaron P, Servais P (1999) Flow cytometric discrimination of bacterial populations based on SYTO 13 staining of nucleic acids. FEMS Microbiol Ecol 29:319–330

Tyndall RL, Hand RE, Mann RC, Evans C, Jernigan R (1985) Application of flow cytometry to detection and characterization of Legionella spp. Appl Environ Microbiol 49:852–857

Yentsch CS, Menzel DW (1963) A method for the determination of phytoplankton chlorophyll and phaeophytin by fluorescence. Deep-Sea Res 10:221–231

UNESCO (1994) Protocols for the Joint Global Ocean Flux Study (JGOFS) core measurements. Manuals and Guides 29:1–170

Vaqué D, Guixa-Boixerau N, Gasol JM, Pedros-Alío C (2002) Distribution of microbial biomass and importance of protists in regulating prokariotic assemblages in three areas close to the Antarctic Peninsula in spring and summer 1995–96. Deep-Sea Res II 49:847–867

Varela M, Fernández E, Serret P (2002) Size-fractionated phytoplankton biomass and primary production in the Gerlache and South Bransfield Straits (Antarctic Peninsula) in austral summer 1995–96. Deep-Sea Res II 49:749–768

Zubkov MV, Fuchs BM, Burkill PH, Amann R (2001) Comparison of cellular and biomass specific activities of dominant bacterioplankton groups in stratified waters of the Celtic Sea. Appl Environ Microbiol 67:5210–5218

Zweifel UL, Hagström A (1995) Total counts of marine bacteria include a large fraction of non-nucleoid-containing bacteria (ghosts). Appl Environ Microbiol 61:2180–2185